Modelling cathode spots in glow discharges in the cathode boundary layer geometry with COMSOL Multiphysics

P. G. C. Almeida, M. S. Benilov, and M. S. Bieniek

Departamento de Física, CCCEE, Universidade da Madeira, Largo do Município, 9000 Funchal, Portugal and Instituto de Plasmas e Fusão Nuclear, Instituto Superior Técnico, Universidade de Lisboa, Portugal

Self-organized cathode spots and patterns in glow discharges are computed for the cathode boundary layer geometry, which is the one employed in most of the experiments reported in the literature. The model comprises conservation and transport equations of electrons and a single ion species, written in the drift-diffusion and local-field approximations, and Poisson's equation. Multiple solutions, existing for the same value of the discharge current and describing modes with different configurations of cathode spots, are computed by means of a stationary solver. One of these solutions is 2D (axially symmetric) and exists for all values of discharge current; termed the fundamental mode. Other computed solutions are 3D, exist in a limited range of discharge currents, and describe modes with different configurations of cathode spots. The computed solutions are compared to their counterparts for the plane-parallel geometry, and experiments. All of the computed modes have been observed in the experiment.

1. Introduction

Self-organization of near cathode spots and patterns in DC glow microdischarges was observed for the first time in 2004 [1] and represents an important and interesting phenomenon. A range of experimental reports have since been published (references in review [2]). Theory exists that describes cathode spots and spot patterns in arc and DC glow discharges and relies on general trends of self-organization in bistable non-linear dissipative systems [2]. The theory is based on the existence of multiple steady-state solutions for the same values of the discharge current and which describe modes of current transfer associated with different spot patterns. The theory has been used with modelling to successfully guide experiments [3]. To date, 3D modelling has been performed for discharges with plane parallel electrodes only (references in [2]), while the vast majority of the experiments have been of cathode boundary layer discharges (CBLD) (references in [2]). CBLD have an electrode geometry consisting of a planar cathode and an anode with a circular opening, separated by a lateral wall as shown in Fig. 1 (cf. Fig. 1 of [3]). In this work, 3D modelling of near-cathode spot and pattern self-organization in CBLD is reported for the first time.

2. Model and numerics

Results reported in this work refer to a discharge in xenon under the pressure of 30Torr. The (only) ionic species considered is Xe_2^+. The numerical model comprises equations for conservation of electrons and ions, written with the drift-diffusion transport approximation, and Poisson's equation. The local-field approximation is employed:

$$\nabla\cdot\mathbf{J}_i = w, \quad \mathbf{J}_i = -D_i\nabla n_i - \mu_i n_i \nabla\varphi,$$
$$\nabla\cdot\mathbf{J}_e = w, \quad \mathbf{J}_e = -D_e\nabla n_e + \mu_e n_e \nabla\varphi,$$
$$\varepsilon_0\nabla^2\varphi = -e(n_i - n_e),$$

where

$$w = n_e\alpha\mu_e E - \beta n_e n_i.$$

Here n_i, n_e, J_i, J_e, D_i, D_e, μ_i, and μ_e are number densities, densities of transport fluxes, diffusion coefficients, and mobilities of the ions and electrons, respectively; α is Townsend's ionization coefficient; β is the coefficient of dissociative recombination; φ is electric potential; $E = |\nabla\varphi|$ is the electric field strength; ε_0 is the permittivity of free space; e is the elementary charge. The Townsend ionization coefficient was evaluated by means of formula:

$$\alpha = Cp\exp\left[-D(p/E)^{1/2}\right].$$

Values of constants C and D were taken from [4] and are 6.53×10^3 $\mathrm{m^{-1}Torr^{-1}}$ and 3.61×10^2 $\mathrm{V^{-1/2}\,(Torr\,m)^{-1/2}}$ respectively. The rate coefficient of dissociative recombination was set equal to $2\times10^{-13}\mathrm{m^3s^{-1}}$. Mobilities were estimated using the formulae $\mu_e = 5.4\times10^{23}/n_n$ $\mathrm{m^{-1}V^{-1}s^{-1}}$ and $\mu_i = 2.1\times10^{21}/n_n$ $\mathrm{m^{-1}V^{-1}s^{-1}}$, where n_n is the neutral gas density. Diffusion coefficients of the ions and the electrons were evaluated with the use of Einstein's relation with the gas and electron temperatures equal to 300K and 1eV respectively.

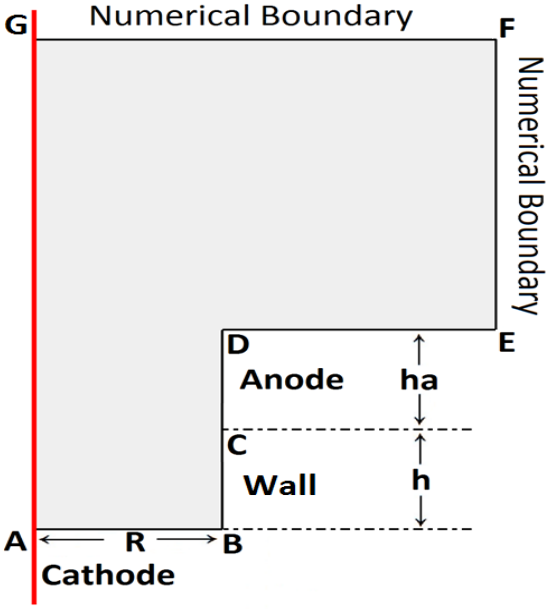

Fig. 1: Cathode boundary layer discharge configuration

Fig.1 shows the discharge configuration. Boundary conditions at the cathode and anode are written in the conventional form: diffusion fluxes of the attracted particles are neglected as compared to drift; the normal flux of the electrons emitted by the cathode is related to the flux of incident ions in terms of the effective secondary emission coefficient [4], which was set equal to 0.03; density of ions vanishes at the anode; electrostatic potentials of both electrodes are given. The lateral wall has the condition of zero normal electric current density. Two boundary conditions are used at the surface of the lateral wall, cases i) where charged species are reflected (normal derivative of charged particle densities set to zero), and ii) where charged species are absorbed (charged particle densities set to zero).

The modes were computed by means of a stationary solver, this allowed a systematic computation and investigation of different modes mapping a current voltage characteristic (CVC). (Note that conventional time-dependent solvers are not fit for this purpose [2].) The stationary-solver used in this work is from the commercial product COMSOL Multiphysics. The input parameter used in the model was discharge voltage or the discharge current, depending on the differential resistance of the discharge. Linear stability analysis is employed to locate bifurcation points, the process discussed in full elsewhere [2]. A 3D calculation domain sector is created by rotation of the domain in Fig. 1 with half the azimuthal angle of the mode being sought. The bifurcation point and subsequent 3D mode is

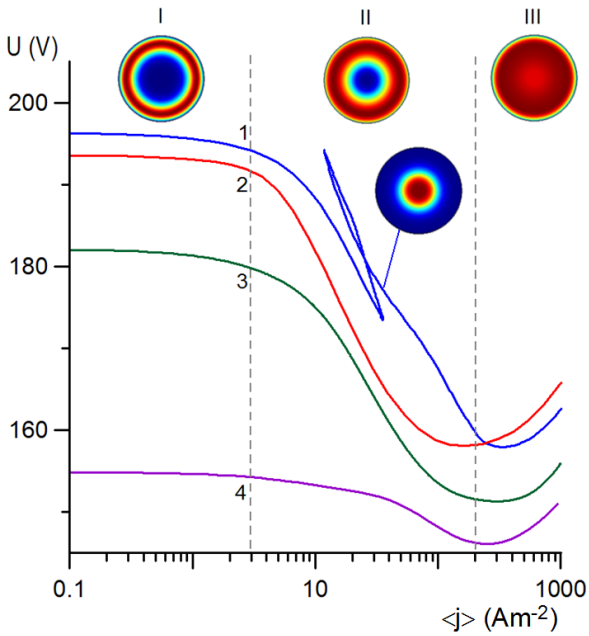

Fig. 2: Fundamental modes, Xenon, 30Torr. Various cathode boundary layer configurations. 1: *h*=0.5 mm, *ha*=0.1 mm, *R*=0.5 mm, absorbing lateral wall. 2: *h*=0.5 mm, *ha*=0.1 mm, *R*=1.5 mm, absorbing lateral wall. 3: *h*=0.5 mm, *ha*=0.1 mm, *R*=0.5 mm, reflecting lateral wall. 4: *h*=0.25 mm, *ha*=0.25 mm, *R*=0.375 mm, absorbing lateral wall.

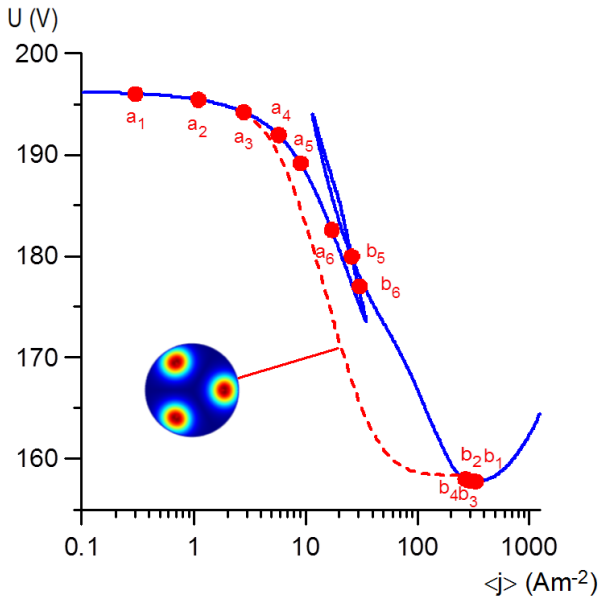

Fig. 3: CVC, xenon, 30 Torr. Solid: Fundamental mode 1 of Fig. 2. Circles: points of bifurcation. Dashed: mode a_3b_3.

then searched for on the fundamental mode for the values of the control parameters predicted by the linear stability analysis.

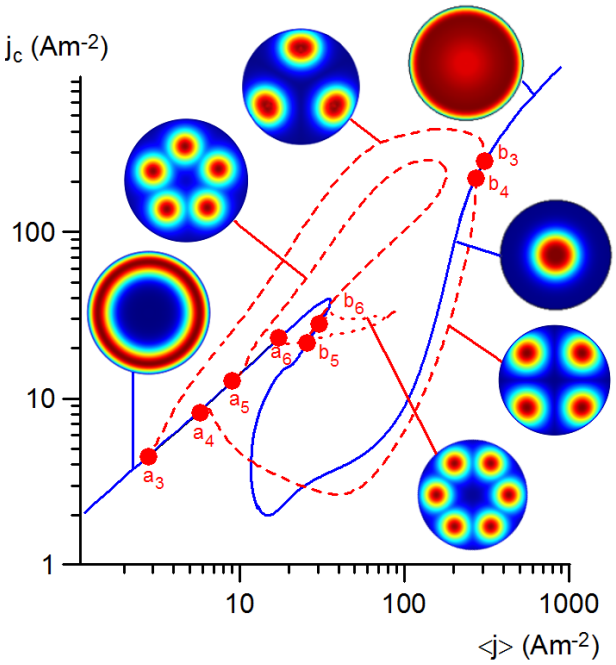

Fig. 4: Bifurcation diagram, xenon, 30 Torr. h=0.5mm, ha=0.1mm, R=0.5mm , absorbing lateral wall. Solid: fundamental mode. Dashed: a_3b_3, a_4b_4, a_5b_5. Dotted: a_6b_6.Circles: points of bifurcation.

3. Results

In Fig. 2, fundamental modes for various conditions are displayed as CVC. These CVC, marked 1-4, map the plane (<j>,U), where <j> is the average current density across the cathode surface and U is the discharge voltage. Illustrated are distributions of current density on the cathode surface, which are characteristic for the given mode in a certain current range. The figure is divided into three ranges of current. Range I, the Townsend discharge, the current is distributed on the cathode in the form of a ring. Range II, the ring of current becomes thicker with increasing current. Range III, the abnormal discharge, the ring has grown and fills most of the cathode surface; here current density increases with increasing current. Mode 1 transits from a current distribution on the cathode of a ring into a central spot, the transition occurs as the current is increased and is associated with a loop in the CVC. A characteristic spot is shown on the schematic connected to mode 1, this applies to the section of the fundamental mode spanning the second (from low currents) section of CVC with a negative differential resistance. Mode 2 has the same conditions as mode 1 except for a larger radius. This prevents the aforementioned transition from ring to central spot. Mode 3 has the same geometry as mode 1, but the wall reflects charged species. This also prevents the transition. Mode 4 has the same geometry as the experimental setup [5], where self-organized patterns had been seen. Modes 1,2 and 4 (the ones with absorbing lateral walls) have a CVC hump in range I, although this cannot be seen in the figure. These modes are the analogue of the well-known von Engel and Steenbeck 1D solution, which is essentially the fundamental mode for parallel plane electrode geometry with reflecting lateral walls.

In Fig. 3, mode 1 from Fig. 2 and a non-fundamental 3D mode are displayed. The schematic in this figure illustrates the pattern of spots associated with each mode. Shown too are points of bifurcation found using linear stability analysis: a_i and b_i designate bifurcation points from where a mode branches off from and rejoins the fundamental mode with an azimuthal period of $2\pi/i$, i.e modes branching from a_1, a_2, a_3, ... have 3D azimuthal periods of 2π, π, $2\pi/3$, ... These modes possess patterns comprising 1, 2, 3, ... spots respectively. Bifurcation points b_1 to b_4 virtually coincide. Points b_5 and b_6 are positioned on the solid line between the sharp turning points. All of the bifurcations occur in range II, but not in the section of the fundamental mode where a central spot is present. The appearance of the bifurcations ordered by azimuthal periodicity as the fundamental mode is followed from low to high currents conforms to previous modelling of discharges with parallel plane electrodes [2]. The CVC of mode a_3b_3 manifests a plateau between 60 Am^{-2} and 120 Am^{-2}, in a similar way as in modes found previously with an absorbing lateral wall [2].

The plane (<j>,U) is not optimal for displaying multiple modes. In Fig. 4 four non-fundamental modes are mapped in the plane (<j>, j_c) where j_c is current density measured at point R = 0.4, θ = 0, where the cathode current density is largest for the Townsend discharge; the obtained map is a bifurcation diagram. One can observe the transition of the fundamental mode from a ring into a central spot by following the mode from low to high currents. Current density j_c decreases while the central spot is forming, then it increases as the ring mode forms, thus yielding a limp Z-shape on the bifurcation diagram. Modes a_5b_5, a_6b_6 experience turning points, or hysteresis. The displayed 3D modes are examples rather than an exhaustive list of possible modes for these conditions.

In Fig. 5 the evolution of patterns for the modes a_3b_3, a_4b_4 a_5b_5, a_6b_6 from Fig. 4, is shown. Let us consider first the evolution of the patterns for mode

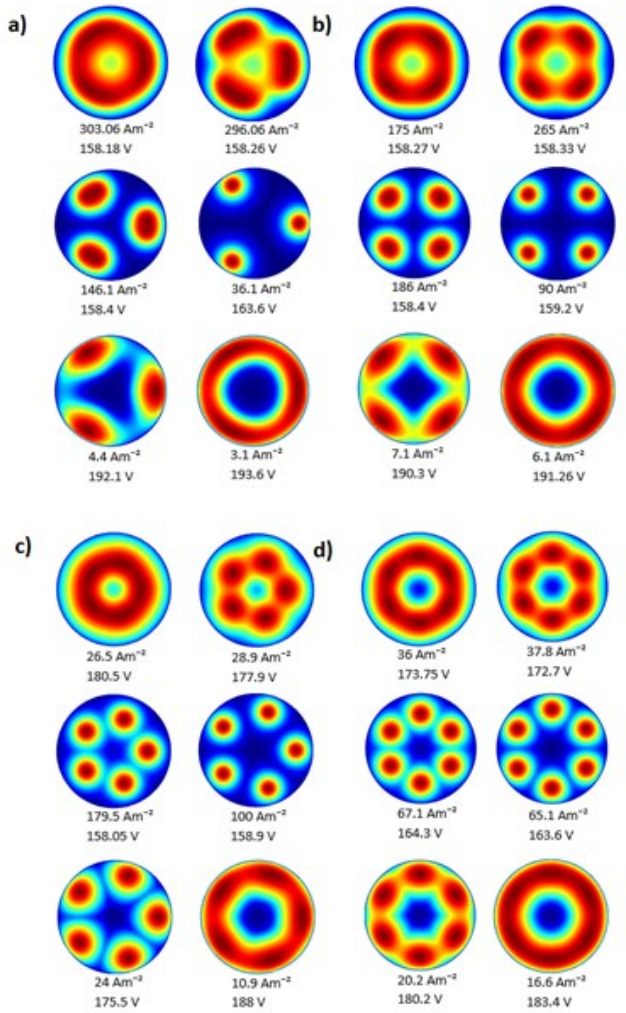

Fig. 5: Evolution of cathode current distributions along a) the 3rd 3D mode b) the 4th 3D mode c) the 5th 3D mode d) the 6th 3D mode.

a_3b_3 which is shown in Fig. 5a). The state 158.18 V is positioned in the vicinity of the bifurcation point a_3, the pattern is of three diffuse elongated spots, slightly deforming a ring pattern into more a triangular type structure. At 158.26 V the three spots have moved away from each other and become more distinct, intense and bean shaped; a trend continuing on to state 158.4 V. At 163.6 V, the spots are farther still from the centre of the cathode. The spots have become circles, which is typically the shape of spots observed in experiments. At 192.1 V a central triangle shaped 'cold spot' is present. The triangle shaped region's points grow less sharp, and the pattern more ring-shaped the closer the mode is to b_3. Fig. 5a, b, c, and d each show a transition from the fundamental mode with a ring at one bifurcation point, to the fundamental mode at another bifurcation point with a ring of a different thickness and radius. The transition occurs first by elongated and then circular spots, the spots then migrate to a different radius, and there they form another, different, ring. No modes with central hot spots were found in the present work, while in previous modelling they were. The images in Fig. 5 of current density can be compared to photos of cathodes from experiments, Fig. 2 of [5], and they are qualitatively the same.

4. Conclusions

Self-organized 3D spot modes have been computed in the cathode boundary layer discharge geometry. This is the first time that such calculations are performed for a geometry different from the parallel-plane one. The pattern of self-organization found is similar to that found in parallel-plane discharges. This finding is consistent with the experimental evidence of such similarity [6]. Furthermore, simulations of 3D spots in a discharge vessel with the lateral wall that fully absorbs the charged particles has been performed for the first time. All the patterns computed in this work and shown in Fig. 5 have been observed in the experiments, cf. Fig. 2 of [5]. The qualitative agreement between the modelling and the experiment is quite good.

Acknowledgments

The work was supported by FCT - Fundação para a Ciência e a Tecnologia of Portugal through the projects PTDC/FIS-PLA/2708/2012 and Pest-OE/UID/FIS/50010/2013.

References

[1] K. H. Schoenbach, *Plasma Sources Sci. Technol.* **13** (2004) 177.

[2] M. S. Benilov, *Plasma Sources Sci. Technol.* **23** (2014) 054019.

[3] W. Zhu et al, *Plasma Sources Sci. Technol.* **23** (2014) 054012.

[4] Yu. P. Raizer, *Gas Discharge Physics* (Berlin, Springer, 1991).

[5] W. Zhu, P. Niraula, *Plasma Sources Sci. Technol.* **23** (2014) 054011.

[6] N. Takano, K. Schoenbach, *Abstracts of the 2006 IEEE Int. Conf. Plasma Sci. (Traverse City, MI)* 247.

[7] P. G. C. Almeida, M. S. Benilov, *Phys. Plasmas* **20** (2013) 101613.